Adsorption (2007) 13: 385–397
DOI 10.1007/s10450-007-9018-4

Reversible chemisorption of carbon dioxide: simultaneous production of fuel-cell grade H_2 and compressed CO_2 from synthesis gas

K.B. Lee · M.G. Beaver · H.S. Caram · S. Sircar

Received: 19 April 2007 / Revised: 8 July 2007 / Accepted: 11 July 2007 / Published online: 14 September 2007

Abstract One vision of clean energy for the future is to produce hydrogen from coal in an ultra-clean plant. The conventional route consists of reacting the coal gasification product (after removal of trace impurities) with steam in a water gas shift (WGS) reactor to convert CO to CO_2 and H_2, followed by purification of the effluent gas in a pressure swing adsorption (PSA) unit to produce a high purity hydrogen product. PSA processes can also be designed to produce a CO_2 by-product at ambient pressure. This work proposes a novel concept called "Thermal Swing Sorption Enhanced Reaction (TSSER)" which simultaneously carries out the WGS reaction and the removal of CO_2 from the reaction zone by using a CO_2 chemisorbent in a single unit operation. The concept directly produces a fuel-cell grade H_2 and compressed CO_2 as a by-product gas. Removal of CO_2 from the reaction zone circumvents the equilibrium limitations of the reversible WGS reaction and enhances its forward rate of reaction. Recently measured sorption-desorption characteristics of two novel, reversible CO_2 chemisorbents (K_2CO_3 promoted hydrotalcite and Na_2O promoted alumina) are reviewed and the simulated performance of the proposed TSSER concept using the promoted hydrotalcite as the chemisorbent is reported.

Keywords Thermal swing sorption enhanced reaction · Chemisorption · Hydrogen · Carbon dioxide · Promoted hydrotalcite · Promoted alumina

1 Introduction

Production of hydrogen by gasification of coal is a commercial technology. It involves high pressure partial oxidation of coal with oxygen and steam to produce a synthesis gas containing CO, CO_2, H_2O, H_2 and trace amounts of H_2S and COS if the coal contained any sulfur. The impurities are removed and the clean gas is subjected to catalytic water gas shift (WGS) reaction [$CO + H_2O \leftrightarrow CO_2 + H_2$] for converting most of the CO to H_2. Finally, the reactor effluent gas is sent to a separation system for production of pure H_2.

Figure 1 is a schematic box diagram of the process concept. A few well known examples of the gasification process include the Shell Coal Gasification Process (Viaswinkel et al. 1997), the Texaco Process (Schlinger et al. 1985) and the Koppers-Totzek Process (Rosen and Scott 1987). New designs of the coal-gasifier continue to be developed (Qunying and Sixun 1997; Stiegel and Ramezan 2003).

The WGS reaction is an equi-molar reaction which is moderately exothermic. The heat of reaction is ~41 kJ/mol of CO. The reversible reaction is thermodynamically controlled. Thus, according to the Le Chatelier's principle, the conversion of CO to H_2 is preferred at a lower temperature, and the gas pressure has no effect on the reaction equilibrium. However, the reaction rate decreases when both the reaction temperature and the pressure are decreased (Rase 1977).

Table 1 shows the equilibrium constants [$K = (y^*_{CO_2} \cdot y^*_{H_2})/(y^*_{CO} \cdot y^*_{H_2O})$] and the specific reaction rate constants [k] for the WGS reaction [on copper-zinc catalyst at a gas pressure greater than 20 atm] as functions of temperature (Rase 1977). It can be shown using the K values of Table 1 that the equilibrium gas phase composition [mole fraction of component $i = y^*_i$] in a batch reactor undergoing the WGS reaction will be a mixture of CO_2, CO, H_2O, and H_2. For

---

K.B. Lee · M.G. Beaver · H.S. Caram · S. Sircar (✉)
Chemical Engineering Department, Lehigh University,
Bethlehem, PA 18015, USA
e-mail: sircar@aol.com

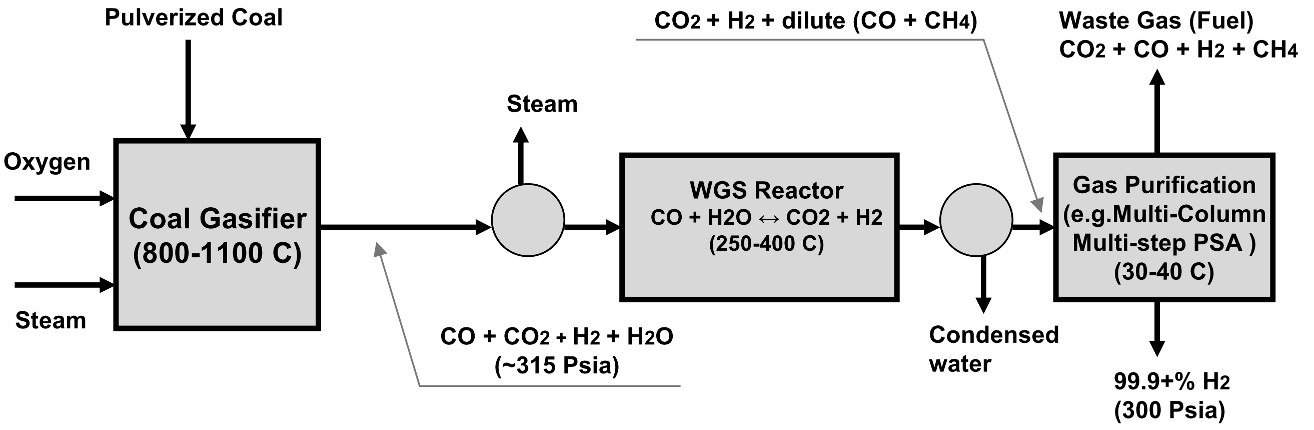

Fig. 1 Schematic box diagram of a conventional process for production of H_2 by coal gasification

Table 1 Characteristics of water gas shift reaction at different temperatures

Temperature (°C)	Equilibrium constant, K	Rate constant, k at 20 atm[a] (Scft/ft^3/hr)
200	335.8	2.67×10^4
250	85.8	4.52×10^4
300	38.6	6.16×10^4
350	20.4	8.00×10^4
400	11.8	9.98×10^4

[a] Copper-zinc catalyst

example, at 400 °C the mixture composition (dry basis) will be 1.345% CO, 49.33% CO_2 and 49.33% H_2 (97.3% conversion of CO to H_2) if a feed gas containing 20% CO + 80% H_2O was initially introduced to the reactor. This gas mixture from the reactor must then be purified to produce a pure H_2 product gas.

Many different separation processes are commercially available for purification of the WGS reactor effluent gas which typically contains CO_2, CO, H_2, H_2O and dilute CH_4. The reactor effluent is cooled to near ambient temperature (30–50 °C) to condense out most of the water and then it is subjected to a purification scheme. The three main purification routes include (a) absorption of CO_2 by a physical (e.g. selexol or rectisol) or chemical solvent (e.g. mono or diethanolamine) (Karasaki et al. 1995; Mimura et al. 1995; IEA Greenhouse Gas R&D Programme 1990; Chakravarti et al. 2001), (b) adsorption of CO_2 and other impurities by a physical adsorbent (e.g. activated carbon and zeolite) (Fuderer and Rudelstorfer 1976; Sircar, 1979, 1988; Sircar and Kratz 1988; Chue et al. 1995), and (c) separation by a membrane (e.g. polymeric) (Koros and Chern 1987; Leci and Goldthorpe 1992; Matsumoto et al. 1992).

The pressure swing adsorption (PSA) process route is often the preferred method of separation for this application because it can directly produce 99.99+% H_2 by removing all of the impurities (CO, CO_2 and H_2O) from the reactor effluent gas in a single unit, and it is a dry process (Fuderer and Rudelstorfer 1976). PSA processes have also been designed to simultaneously produce a pure H_2 product stream at feed gas pressure and an essentially pure CO_2 product stream at near ambient pressure (Sircar 1979; Sircar and Kratz 1988). All PSA processes, however, operate at near ambient temperature. The solvent absorption routes only remove CO_2. They can be corrosive and energy intensive. Membrane processes are generally not suitable for production of high purity products.

A recent technical report entitled “The Hydrogen Economy: Opportunities, Costs, Barriers and R&D Needs”, which was published by the US National Research Council and National Academy of Engineering (2004), emphasizes the “capture and storage of CO_2 by-product of H_2 production from coal” as one of the R&D priorities among others. Consequently it will be highly desirable if an intensified process concept can be developed which combines the water gas shift reaction and the subsequent CO_2 separation from the reaction product in a single unit operation for simultaneous production of essentially pure CO_2 and H_2 products, both at feed gas pressures. Development of such “one-box” process will have the following major advantages over the conventional methods of H_2 production outlined earlier:

- Removal of CO_2 from the reaction zone of the WGS reactor will drive the WGS reaction forward according to the Le Chatelier’s principle. This will permit (i) higher conversion of CO to H_2 than that governed by the thermodynamic equilibrium, (ii) enhancement of the forward reaction rate, (iii) the use of a lower H_2O/CO ratio in the feed gas, and (iv) relatively higher temperature operation of the reactor without the thermodynamic penalty.

- The concept will also permit direct production of CO_x free H_2 from the reactor at feed gas pressure which eliminates any subsequent separation process need.
- Simultaneous production of an essentially pure and compressed CO_2 by-product will facilitate (i) subsequent CO_2 sequestration (elimination of green house gas emission) or (ii) sale of CO_2 product.
- Potential for significant savings in capital and energy costs due to simpler equipments, absence of high temperature metallurgical demands, elimination of separate product purification unit, and small foot print of the over all process.

2 Novel Thermal Swing Sorption Enhanced Reaction (TSSER) concept

We propose the development of a novel concept called "Thermal Swing Sorption Enhanced Reaction (TSSER)", which will satisfy all of the goals mentioned above. The process will have the following five cyclic sequential steps:

- *(a) Sorption enhanced reaction step*: A feed gas containing a mixture of CO and H_2O at a temperature of T_R and a total gas pressure of P_R is passed through a sorber-reactor column packed with an admixture of a WGS reaction catalyst and a high temperature CO_2 selective sorbent. The sorber-reactor is filled with steam at temperature T_R and pressure P_R prior to this step. CO and H_2O react to form CO_2 and H_2. CO_2 is removed from the reaction zone by the sorbent and an essentially CO_x free product gas containing H_2 and H_2O is produced at pressure P_R as the reactor effluent. A H_2 enriched product (∼99.99+%) is then produced at feed pressure by condensing out the water from the reactor effluent by cooling. The step is continued until the chemisorbent in the sorber-reactor is nearly saturated with CO_2 (short of CO_x breakthrough).
- *(b) CO_2 purge step*: The sorber-reactor is co-currently purged with a stream of essentially pure CO_2 at pressure P_R and temperature T_R to purge out the left-over void gas from the sorber-reactor at the end of step (a). Some additional CO_2 is sorbed. The effluent gas may be rejected or recycled by mixing it with fresh feed gas to step (a). The chemisorbent is saturated with essentially pure CO_2 at pressure P_R at the end of this step.
- *(c) Batch heating step*: The column is heated indirectly to a temperature of T_H ($>T_R$) in a batch fashion by raising the shell side temperature to T_H. The column pressure rises to P_H ($\gg P_R$) due to batch desorption of CO_2. The column is saturated with pure CO_2 at pressure P_H and temperature T_H at the end of this step.
- *(d) Regeneration by high pressure steam purge step*: The sorber-reactor is counter-currently purged with super-heated steam at pressure P_H and temperature T_H until a certain amount of the CO_2 is desorbed out of the column. The effluent gas is initially pure CO_2 at pressure P_H, followed by a mixture of CO_2 and steam with decreasing partial pressures of CO_2. The water is condensed out from the effluent gas by cooling in a constant pressure condenser. This produces a CO_2 enriched (∼99.9+%) product gas at pressure P_H.
- *(e) Multi-tasking regeneration step*: The sorber-reactor pressure is reduced to a near ambient pressure level and counter-currently purged with super-heated steam at temperature T_R, while lowering the shell side temperature to T_R, until most (>95%) of the CO_2 is removed from the column. The effluent gas is rejected. The column is cooled down to T_R at the end of this step and the column pressure is raised from near ambient to P_R by counter-currently introducing steam into the column at temperature T_R and pressure P_R. The cycle is then repeated starting from step (a).

Shell and tube-type heat exchangers may be used as the sorber-reactors (see insert in Fig. 2) for the process. The tube sides will be packed with an admixture of the WGS catalyst and the CO_2 sorbent. The shell sides will be used for flowing the heating and cooling fluids (e.g. steam) for indirect heating and cooling of the tubes. A cross flow heat exchanger where super-heated steam is used as the heating medium in the shell side may be preferred. At least four parallel sorber-reactors are used to operate the above-described five-step cyclic process in a continuous manner as shown by Fig. 2. Table 2 shows an example of the operation scheme for a four sorber-reactor embodiment of the proposed process concept. It is designed to allow continuous introduction of the reactants (synthesis gas) to the system, continuous production of H_2 product, and continuous production of the CO_2 by-product.

The key functions of the individual steps of the proposed TSSER process are given below:

- Step (a) circumvents the thermodynamic limitation of the reversible WGS reaction, thereby achieving nearly complete conversion of CO to H_2 and direct production of fuel-cell grade H_2 (dry basis) at reaction pressure in a single unit operation.
- Step (b) replaces the sorber-reactor void gas impurities at the end of step (a) by essentially pure CO_2 which facilitates production of pure CO_2 by-product in step (d).
- Step (c) permits in situ compression of CO_2 inside the sorber-reactor to a pressure much higher than the reactor feed pressure by thermal desorption of CO_2 which permits the production of compressed by-product CO_2 in step (d).

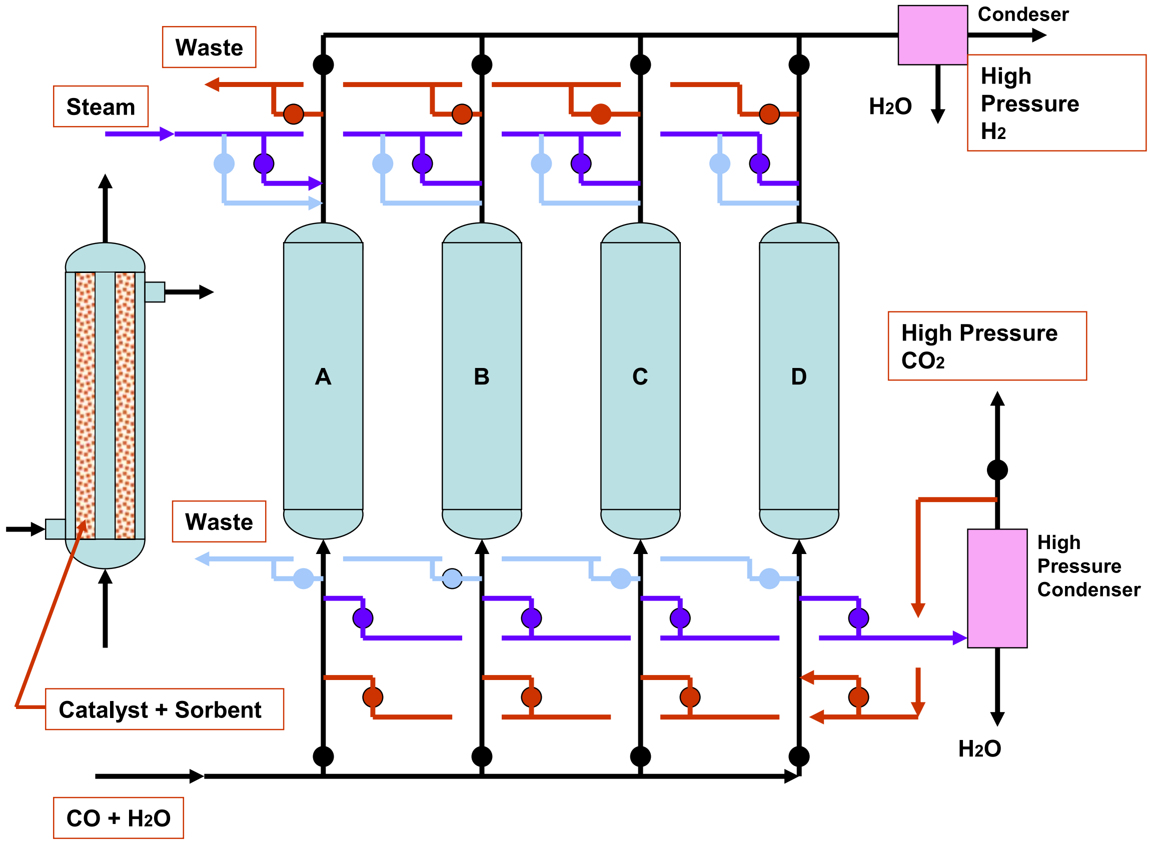

Fig. 2 Schematic drawing of the SER process embodiment for simultaneous production of CO_2 and H_2 from synthesis gas

Table 2 Example of the operation scheme for the steps of the SER process[a]

<table>
<tr><td>Column A</td><td colspan="2">SR (H₂ Product)</td><td>R</td><td colspan="2">BH</td><td colspan="2">HPP (CO₂ Product)</td><td>D/C/LPP/P</td></tr>
<tr><td>Column B</td><td>HPP</td><td>D/C/LPP/P</td><td colspan="2">SR (H₂ Product)</td><td>R</td><td colspan="2">BH</td><td>HPP</td></tr>
<tr><td>Column C</td><td>BH</td><td colspan="2">HPP (CO₂ Product)</td><td>D/C/LPP/P</td><td colspan="2">SR (H₂ Product)</td><td>R</td><td>BH</td></tr>
<tr><td>Column D</td><td>R</td><td colspan="2">BH</td><td colspan="2">HPP (CO₂ Product)</td><td>D/C/LPP/P</td><td colspan="2">SR (H₂ Product)</td></tr>
</table>

[a] SR—sorption reaction, R—CO_2 rinse, BH—batch heating, HPP—high pressure steam purge, D—depressurization, C—cooling, LPP—low pressure steam purge, P—pressurization

- Step (d) allows simultaneous production of compressed high purity CO_2 by-product (dry basis). It also partially and efficiently regenerates the chemisorbent by using the principle of thermal swing sorption.
- Step (e) serves many purposes including (i) very efficient final regeneration of the sorbent, requiring relatively small amount of steam, and (ii) preparation of the sorber-reactor to begin a new cycle.

These individual functions of the steps of the TSSER process result in (i) very high cyclic CO_2 working capacity, (ii) low net steam consumption for regeneration, and (iii) compact and small foot-print process design.

3 Reversible chemisorption of carbon dioxide for the TSSER concept

A critical requirement for the above-described TSSER process is the availability of a CO_2 selective sorbent which can reversibly and selectively remove CO_2 from the reaction zone of the WGS reactor in presence of H_2O, CO, and H_2 at the WGS reaction temperature of 250–400 °C. The sorbent

Fig. 3 CO_2 chemisorption isotherms on K_2CO_3 promoted hydrotalcite

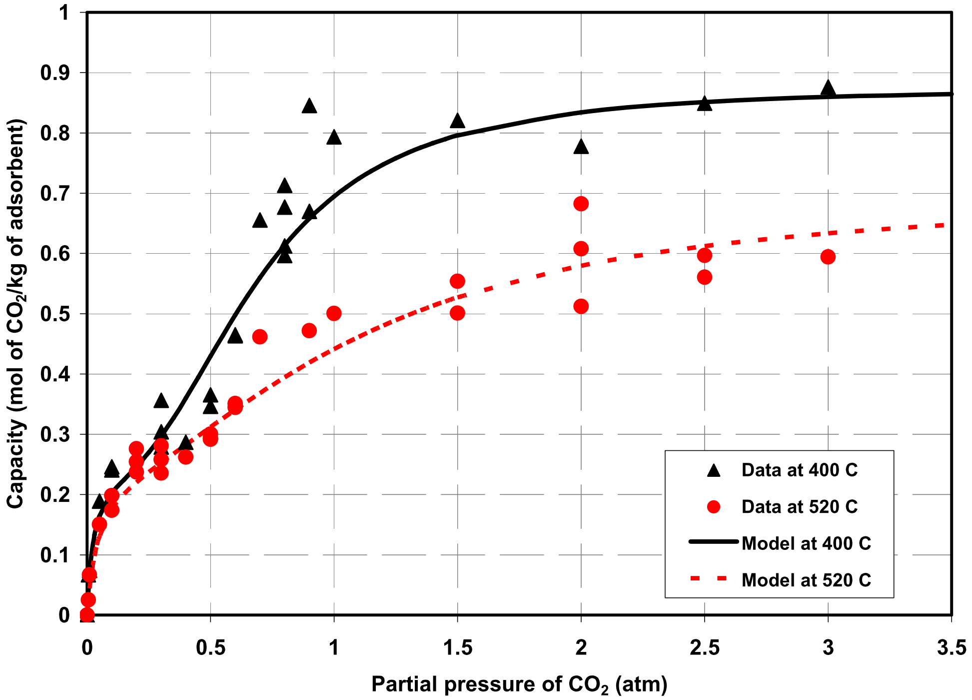

must also exhibit (a) acceptable cyclic working capacity for CO_2 sorption in presence of steam, (b) relatively fast sorption and desorption kinetics for CO_2, (c) moderate heat of sorption of CO_2, and (d) thermal stability at the reaction condition.

It is imperative that conventional CO_2 physisorbents like zeolites or activated carbons can not be employed for this application because of their low sorption capacities at elevated temperatures (>300 °C) and poor selectivities in presence of steam. Reversible CO_2 selective chemisorbents, which satisfy the above-described properties, will be necessary. Fortunately, two such novel materials have been identified. They are (a) K_2CO_3 promoted hydrotalcite, and (b) Na_2O promoted alumina. Both materials were originally developed by Air Products, Inc., and donated to the Lehigh University for further development. The promoted hydrotalcite was previously used for the development of a pressure swing sorption enhanced reaction process (PSSER) concept for production of fuel-cell grade H_2 by low temperature (~450 °C instead of conventional 900 °C) steam reforming of methane (Hufton et al., 1999, 2000; Sircar et al. 2000; Waldron et al. 2001). It was also used recently to develop a TSSER concept for the same application (Lee et al. 2007a). The promoted alumina was previously used for the development of a high temperature PSA process for removal of CO_2 from a waste gas without pre-drying (Sircar and Golden 2001). Both materials were extensively tested for their thermal stability (Hufton et al. 1999; Sircar and Golden 2001).

Extensive measurement of pure CO_2 sorption capacities, sorption kinetics, and column dynamics for CO_2 sorption and desorption on samples of these two chemisorbents at different temperatures and pressures were recently carried out using a column apparatus (Lee et al., 2007b, 2007c). These properties were used in the simulation of the above-described TSSER concept for simultaneous production of fuel-cell grade H_2 and compressed CO_2 from a synthesis gas. Some of these findings are reported below:

4 CO_2 chemisorption isotherms

Figures 3 and 4, respectively, show the equilibrium isotherms for chemisorption of pure CO_2 on the promoted hydrotalcite at 400 and 520 °C (Lee et al. 2007b), and the promoted alumina at 250, 350 and 450 °C (Lee et al. 2007c) in the CO_2 pressure range of 0–3.5 atm.

The CO_2 chemisorption isotherms on both materials obeyed the classic Langmuir model of pure gas chemisorption (5) in the low pressure region, but they both significantly deviated from that model in the higher pressure region. Consequently, a novel equilibrium model was proposed to describe the data of Figs. 3 and 4 (Lee et al., 2007b, 2007c). The model assumed that the following two simultaneous reactions were occurring when a pure gas A was contacted with the chemisorbent:

- Reversible chemisorption of A on the surface of the chemisorbent:

$$\text{A (gas)} + \text{S (empty site)} \leftrightarrow \text{A-S (chemisorbed A)} \qquad (1)$$

Fig. 4 CO_2 chemisorption isotherms on Na_2O promoted alumina

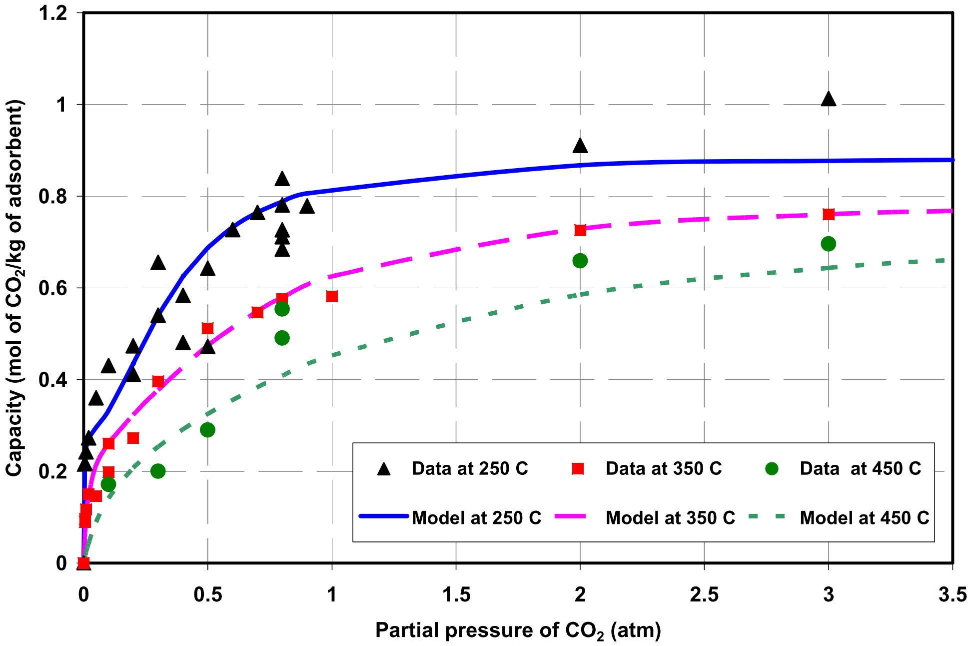

- Reversible chemical complexing between the gas and the chemisorbed molecules of A:

$$\text{aA (gas)} + \text{A-S} \leftrightarrow \text{A}_{(a+1)}\text{-S (surface complex)} \tag{2}$$

Equation (1) describes the classic Langmuirian mechanism of chemisorption where one molecule of a gas A is chemisorbed on one empty chemisorption site of an energetically homogeneous sorbent. The components S and A-S, respectively, represent the empty site and the chemisorbed A molecule. Equation (2) describes the additional complexation reaction between the gas molecules of component A and the chemisorbed A molecules. It was assumed that ‘a’ molecules of gas A reacted with each chemisorbed A molecule to form one molecule of the surface complex $A_{(a+1)}$-S. The over-all equilibrium chemisorption isotherm for the proposed model could be derived as (Lee et al. 2007b):

$$n^*(P,T) = \frac{mK_C P[1+(a+1)K_R P^a]}{[1+K_C P + K_C K_R P^{(a+1)}]} \tag{3}$$

where n^* is the total specific equilibrium amount (mol/kg) of gas A sorbed on the chemisorbent at pressure P (atm) and temperature T (K). The equilibrium parameters of (3), which are functions of temperature only, are given by:

$$K_C = \frac{k_a}{k_d} \quad (\text{atm}^{-1}); \qquad K_R = \frac{k_f}{k_b} \quad (\text{atm}^{-a}) \tag{4}$$

where k_a and k_d are, respectively, the specific rate constants for the chemisorption and desorption reactions on the surface, and k_f and k_b are, respectively, the specific rate constants for the forward and backward surface complexation reactions.

Equation (3) reduces to the Langmuir equation in the low pressure region, and n^* asymptotically approaches $n^m = m(a+1)$ at the limit of $P \to \infty$:

$$n^*(P,T) = \frac{mK_C P}{[1+K_C P]} \quad \text{for small values of P or } n^* \tag{5}$$

The parameters of (3) are m (mol/kg), the saturation chemisorption capacity of the chemisorbent surface; K_C (atm^{-1}), the equilibrium constant for the chemisorption reaction; K_R (atm^{-a}), the equilibrium constant for the additional complexation reaction; and a, the stoichiometric coefficient for the complexation reaction. The thermodynamic constants (K_C and K_R) are exponential functions of temperature (Lee et al. 2007b):

$$\frac{d\ln K_C}{dT} = -\frac{q_C}{RT^2}; \qquad \frac{d\ln K_R}{dT} = -\frac{\Delta H_R}{RT^2} \tag{6}$$

$$K_c = K_c^o \exp[q_C/RT]; \qquad K_R = K_R^o \exp[\Delta H_R/RT] \tag{7}$$

where q_C and ΔH_R (kJ/mol) are, respectively, the molar isosteric heat of chemisorption and the heat of additional surface reaction. K_C^o (atm^{-1}) and K_R^o (atm^{-a}) are constants.

Equation (3) was used to describe the new isotherm data for chemisorption of CO_2 on both of the chemisorbents as shown by Figs. 3 and 4. The solid and dashed lines show the best fit of the data by the model using the parameters given in the Tables 3 and 4 which also report the Henry’s Law constants (K_H) for the isotherms at different temperatures. The fit is very good suggesting that the proposed model is adequate to describe the isotherms.

It may also be seen from Tables 3 and 4 that the heats of CO_2 chemisorption and surface complexation reaction are

Table 3 Model parameters for CO_2 chemisorption on K_2CO_3 promoted hydrotalcite

T (°C)	m (mol/kg)	a	K_C (atm^{-1})	K_R (atm^{-a})	$K_H = mK_C$ (mol/kg/atm)	ΔH_R (kJ/mol)	q_c (kJ/mol)
400	0.25	2.5	37.4	2.5	9.35	42.2	21.0
520	0.25	1.8	21.2	0.8	5.30		

Table 4 Model parameters for CO_2 chemisorption on Na_2O promoted alumina

T (°C)	m (mol/kg)	a	K_C (atm^{-1})	K_R (atm^{-a})	$K_H = mK_C$ (mol/kg/atm)	ΔH_R (kJ/mol)	q_c (kJ/mol)
250	0.295	2.0	536	8	158	37.5	64.9
350	0.295	1.7	48.3	2	14.2		
450	0.295	1.5	8.47	0.73	2.45		

rather moderate (∼20–65 kJ/mol) on both materials, indicating that the chemisorption bond is rather weak. This facilitates ease of desorption of CO_2 from these materials, which is a very desirable property for the TSSER process. The isosteric heat of chemisorption of CO_2 on the promoted alumina was about three times larger than that on the promoted hydrotalcite. On the other hand, the heats of surface complexation on both materials were comparable. These heats were estimated by the best fit of the experimental chemisorption isotherms by the model. It will be necessary to investigate into the chemical nature of the chemisorbed and complexation compounds to understand the cause of the differences in these heats.

5 Column dynamics for CO_2 chemisorption

Figures 5 and 6, respectively, show the column breakthrough data for chemisorption of 60% CO_2 from N_2 at a pressure of 1 atm on the promoted hydrotalcite at 400 °C and the promoted alumina at 350 °C. The column was ∼100 cm long (1.73 cm diameter) and initially free of CO_2 (Lee et al., 2007b, 2007c). The figures plot the ratio of the mole fraction of CO_2 [y(t)] at time t in the column effluent gas to the feed gas CO_2 mole fraction [y_o] as a function of the dimensionless time [t/t*]. The variable t* is the stoichiometric breakthrough time.

It may be seen from Figs. 5 and 6 that the breakthrough curves are nearly vertical, indicating fast kinetics of CO_2 sorption. The tail at the trailing edge of the CO_2 break through curve is a signature of a non-isothermal, non-adiabatic column (Sircar et al. 1983; Lee et al. 2007b, 2007c). The profiles can be simulated well by the classic Linear Driving Force (LDF) Model describing the local rate of CO_2 mass transfer inside the column at distance z and time t [$(\frac{\delta n}{\delta t})_z = k(n^* - n)$], and the chemisorption equilibrium isotherm model of (3). The variables n(z, t) and n*(z, t) are, respectively, the specific local CO_2 loading on the chemisorbent and the corresponding gas phase specific equilibrium CO_2 sorption capacity at z and t. The variable k is the LDF mass transfer coefficient. The CO_2 mass transfer coefficients were found to be rather weak functions of temperature and independent of CO_2 concentration in the mole

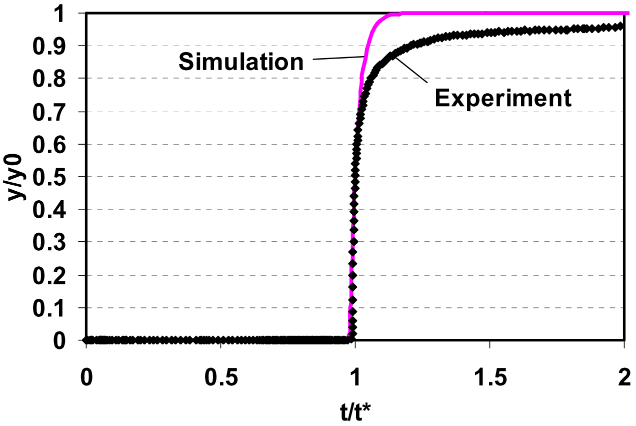

Fig. 5 Column breakthrough profiles for CO_2 on promoted hydrotalcite at 400 °C

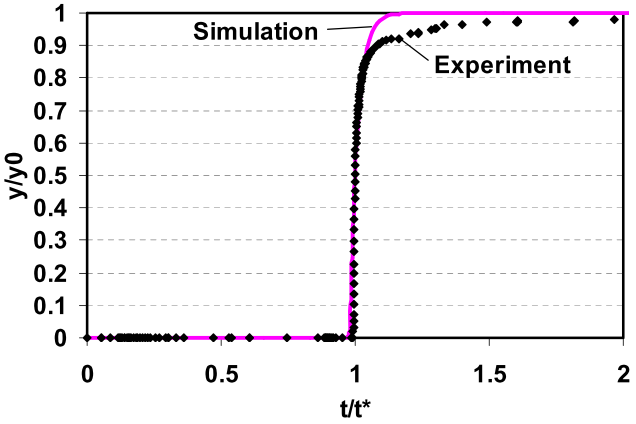

Fig. 6 Column breakthrough profiles for CO_2 on promoted alumina at 350 °C

fraction range of 0.4–0.6 (Lee et al., 2007b, 2007c). Table 5 gives a few examples of the k values at different temperatures (Lee et al., 2007b, 2007c). They have the same order of magnitude for both chemisorbents. However, the coefficients are relatively larger for the promoted alumina than those for the promoted hydrotalcite at the same temperature.

6 Column dynamics of isothermal CO_2 desorption from the chemisorbents

Figures 7 and 8 show the profiles of the fraction of CO_2 desorbed from a column (∼100 cm long) by pure N_2 purge as a function of the cumulative specific amount of N_2 introduced into the column, respectively, for columns packed with promoted hydrotalcite and promoted alumina. The columns were initially equilibrated with 40% CO_2 in N_2 at a total gas pressure of 1 atm and a temperature of 520 °C (promoted hydrotalcite) and 350 °C (promoted alumina). The purge N_2 gas was also at the same temperature and pressure.

Figures 7 and 8 also show the model simulations of the CO_2 desorption characteristics generated using the LDF model for describing CO_2 desorption kinetics with identical values of mass transfer coefficients as CO_2 sorption (Table 5) and the equilibrium chemisorption model of (3). The simulations trace the experimental desorption characteristics very well indicating that there is no difference in CO_2 sorption and desorption mass transfer coefficients for either of the chemisorbents. This is a very important finding. It contradicts the analysis of a previously published study where the CO_2 desorption kinetics on a sample of K_2CO_3 promoted hydrotalcite was found to be much slower than the corresponding sorption kinetics (Ding and Alpay 2000). Variances in the sorbent samples could be a reason for this difference.

Table 5 Examples of CO_2 sorption and desorption mass transfer coefficients

Chemisorbent		LDF mass transfer coefficients for sorption and desorption of CO_2 (min^{-1})
K_2CO_3 promoted hydrotalcite	400 °C	3.0
	520 °C	5.0
Na_2O promoted alumina	250 °C	4.0
	350 °C	5.0

7 Performance simulation of the TSSER process concept

We simulated the performance of the previously-described five-step TSSER process for simultaneous production of fuel-cell grade H_2 and pure compressed CO_2 by-product using an ideal synthesis gas ($CO:H_2O$= 1:4) as the reactor feed (pressure: 15 or 25 atm, temperature: 400 °C). The well-known "CSTR in series" model (Levenspiel 1962) was adapted for dynamic simulation of the sorption-reaction and the thermal regeneration steps of the TSSER process. A detailed description of the mathematical framework of the model and the method of solution can be found elsewhere (Lee et al. 2007a). The key model assumptions included (i) ideal gas behavior, (ii) instantaneous thermal equilibrium between the gas and the solid inside the sorber-reactor tubes, and (iii) absence of axial dispersion and column pressure drop. The ordinary differential equations of the model representing (i) the transient component and the over-all mass balances, and (ii) the transient energy balance including heat transfer from the shell side to the tube side of the sorber-reactor were simultaneously solved using Matlab function ODE15S which is a variable order solver based on the numerical differentiation formulas. It was assumed that the sorber-reactor tube was packed with an admixture of 90% K_2CO_3 promoted hydrotalcite and 10% WGS catalyst (by weight). The shell side of the reactor was maintained at 400 °C during steps (a), (b), and (e) and at 550 °C during steps (c) and (d) of the process. Pure CO_2 was co-currently introduced into the reactor tube at 15 or 25 atm and 400 °C during step (b). Super-heated steam was counter-currently introduced into the reactor tube at 550 °C during step (d) and at 400 °C during step (e). The steam pressures were equal to the prevailing sorber-reactor pressures. The CO_2 chemisorption isotherm and the heats of sorption were described by

Table 6 Physical dimensions and operating conditions of TSSER reactor

Length of a tube in the reactor = 500 cm; diameter of a tube = 1.73 cm
Bulk density of catalyst/chemisorbent admixture = 0.82 g/cm^3
Weight fraction of catalyst in reactor = 0.10
Feed to the reactor: $H_2O:CO$ = 4:1; pressure = 15.0, 25.0 atm; temperature = 400 °C
Times (minutes) for steps: (a) = 10.0, (b) = 1.0, (c) = 10.0, (d) = 10.0, (e) = 9.0
Feed gas (step a) and purge steam (steps d and e) flow rates: 0.157 (15.0 atm case) and 0.166 (25.0 atm case) gmoles/cm^2/minute
CO_2 rinse rate: 0.135 (15.0 atm case) and 0.225 (25.0 atm. case) gmoles/cm^2/minute

Fig. 7 CO_2 desorption characteristic from K_2CO_3 promoted hydrotalcite at 520 °C

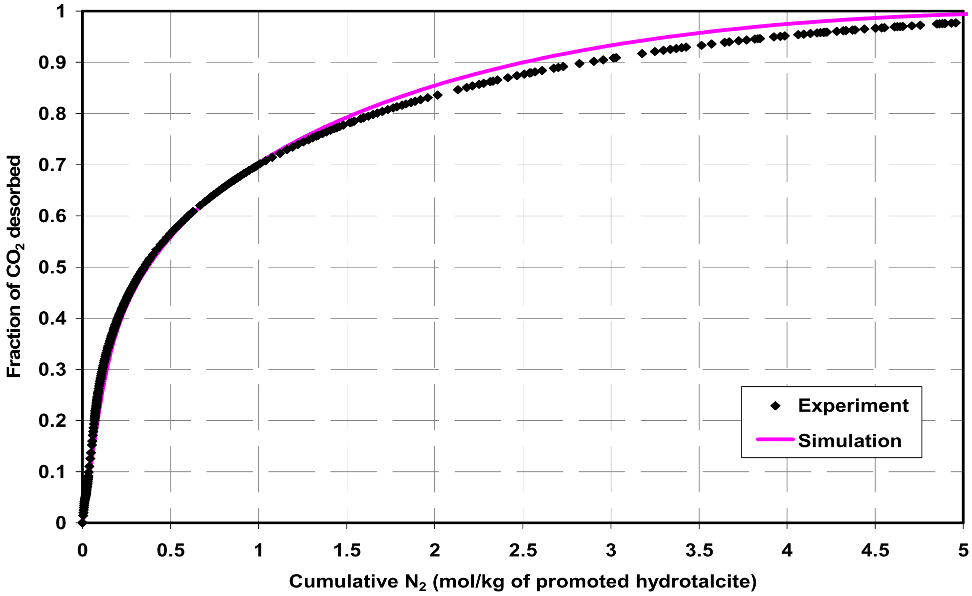

Fig. 8 CO_2 desorption characteristic from Na_2O promoted alumina at 350 °C

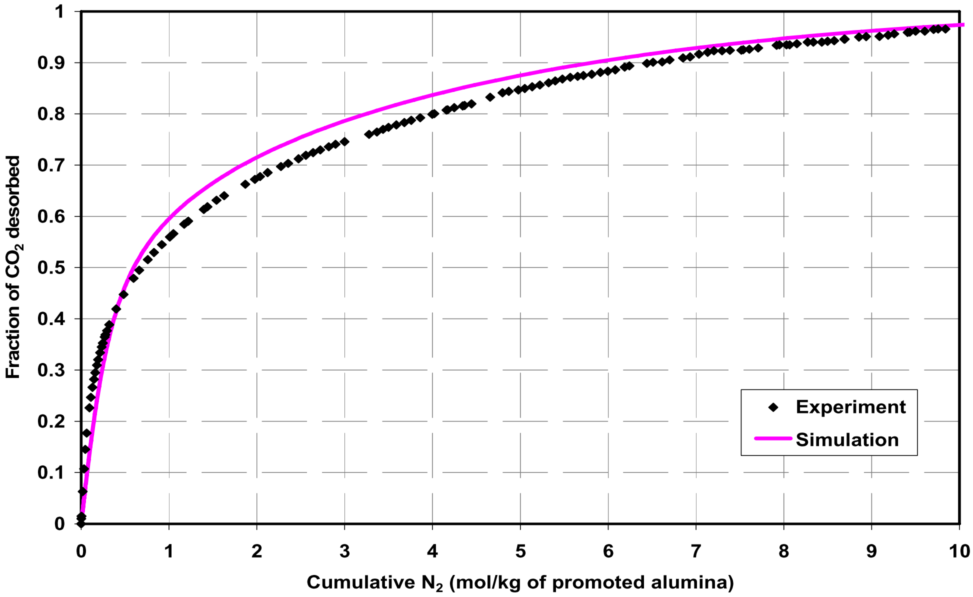

(3) and the parameters of Table 3, the CO_2 chemisorption kinetics was described by the LDF model and the parameters of Table 5, and the kinetics of WGS reaction was described by an empirical model (Xu and Froment 1989; Lee et al. 2007a). The key process design parameters and operating conditions are given in Table 6.

8 Simulation results

A few selected results of the process simulation for the case, where the feed synthesis gas was at 15.0 atm, are described below.

Sorption-reaction step: The feed gas mixture reacts to form CO_2 and H_2. The CO_2 is selectively chemisorbed, which drives the WGS reactions to near completion, thus producing a stream of fuel-cell grade H_2(dry basis) from the sorber-reactor. A reaction-mass transfer zone (RMTZ) is formed near the entrance of the reactor where all of the chemical reactions and the subsequent chemisorption of CO_2 take place. The RMTZ moves forward to the H_2 product end as more feed gas is introduced. The section of the reactor behind the RMTZ remains essentially equilibrated with a gas mixture whose composition is determined by the thermodynamics of the WGS reaction without the chemisorption of CO_2.

Fig. 9 Shape and location of RMTZ inside the sorber-reactor at time t during step (a)

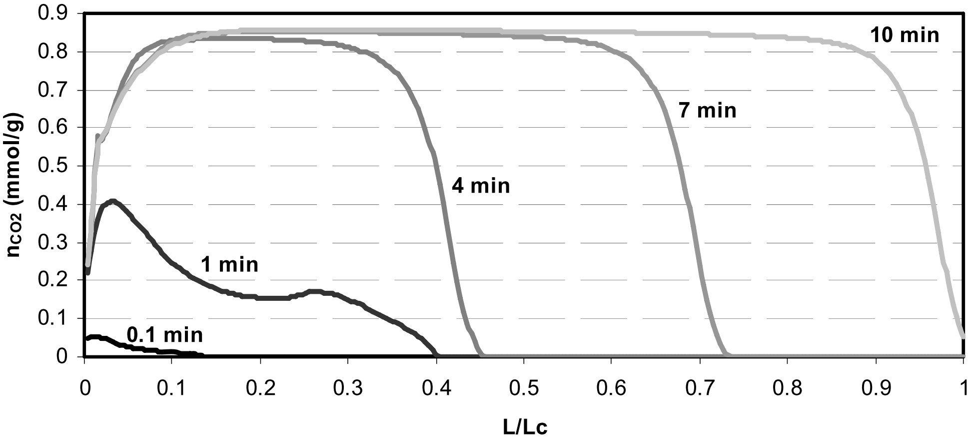

Fig. 10 Temperature profiles inside the sorber-reactor at time t during step (a)

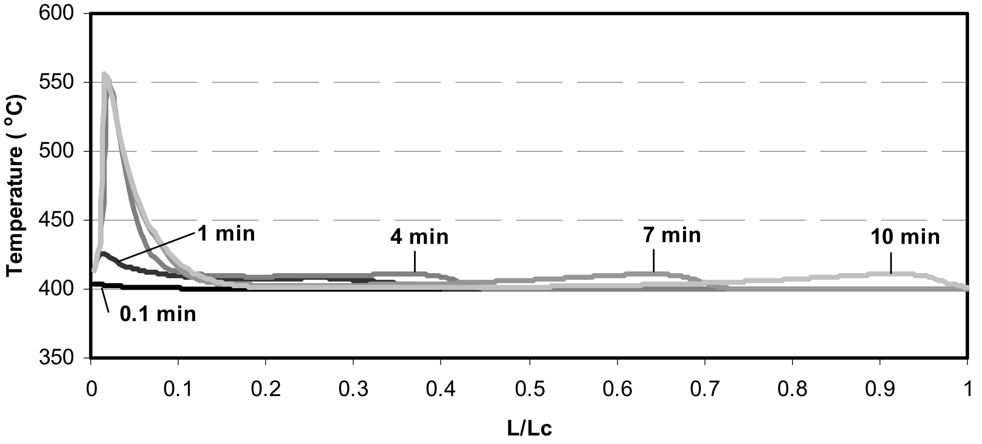

Fig. 11 CO_2 loading profiles inside the sorber-reactor at time t during step (d)

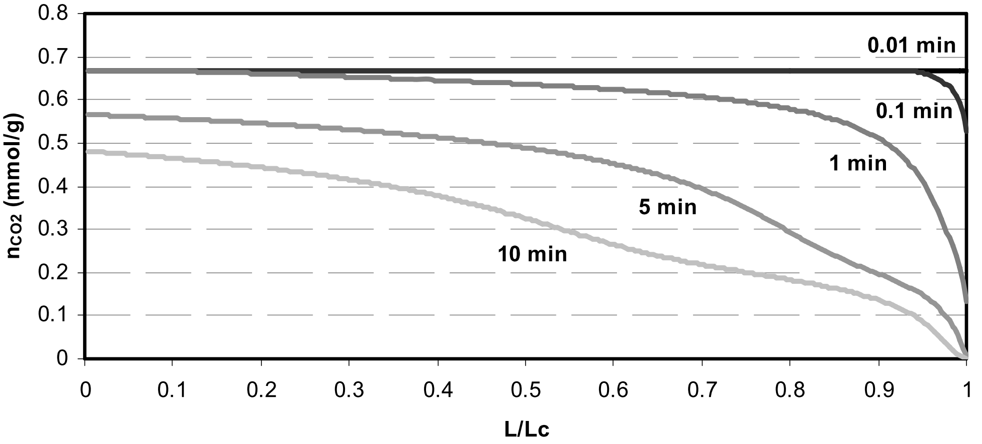

Figure 9 shows the simulated profiles of the RMTZ through the sorber-reactor at different times for the reactor operating conditions given by Table 6. It plots the specific CO_2 loadings on the chemisorbent (mol/kg) as functions of dimensionless distance in the sorber-reactor (L/L_c) at different times. L is the actual distance in the column from the feed end and L_c is the total column length. The sorption-reaction step is stopped at a time of 10 minutes when the leading edge of the RMTZ reaches the reactor- end causing incipient breakthrough of CO_x. The simulated temperature profiles inside the reactor during the sorption-reaction step of the TSSER process are shown by Fig. 10. The reactor feed- end temperature increases to ∼550 °C as soon as the feed gas is introduced due to the release of the heat of exothermic WGS reaction. The column temperature then decreases to the initial temperature of 400 °C in the early

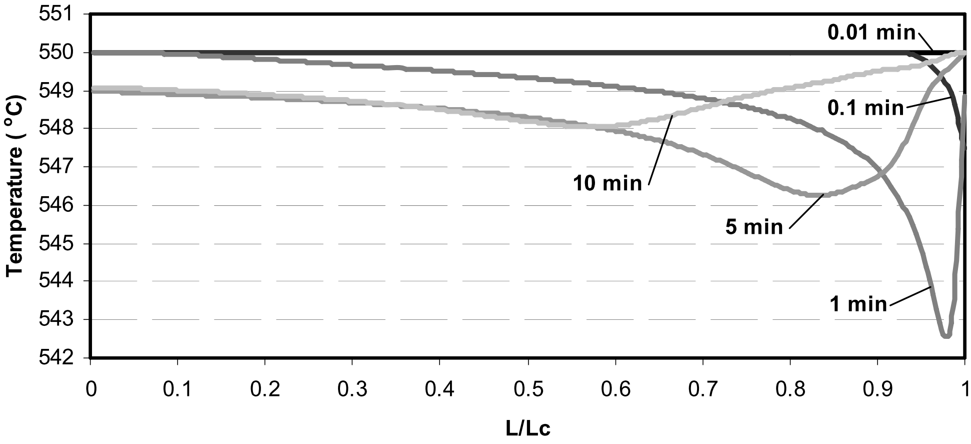

Fig. 12 Temperature profiles inside the sorber-reactor at time t during step (d)

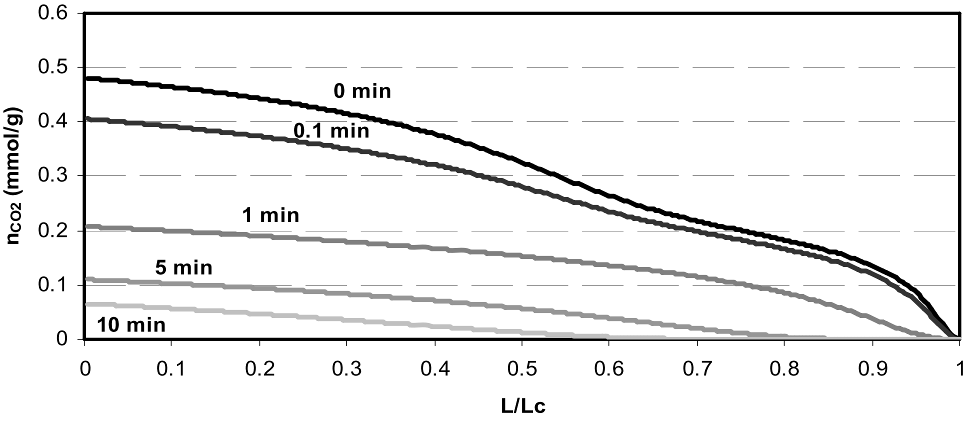

Fig. 13 CO_2 loading profiles inside the sorber-reactor at time t during step (e)

part of the reactor. The size of this heating section increases as more feed gas is introduced but it does not expand beyond ~20% of the reactor length during the entire sorption-reaction step (except progressively small blips in temperature as the CO_2 RMTZ progresses through the column). Most of the conversion of feed CO to H_2 by the WGS reaction occurs in the initial section of the reactor during step (a). The rest of the column is utilized to carry out the rest of the conversion (~100%) and purification of the effluent H_2 product gas to fuel-cell grade (<10 ppm CO).

Figures 11 and 12, respectively, show the simulated specific CO_2 loading profiles on the chemisorbent and the corresponding temperature profiles inside the sorber-reactor at different times during the high pressure steam purge step (d). The chemisorbent is progressively cleaned and an effluent gas containing bulk CO_2 mixed with steam is produced at a much higher than the feed gas pressure. The effluent gas is initially pure CO_2, and then the CO_2 concentration progressively decreases. The water is condensed out in a constant pressure heat exchanger to produce the high pressure CO_2 by-product.

The profiles of Fig. 12 show that the temperature in the H_2 product end of the reactor initially dips by ~7 °C in order to partially supply the heat of CO_2 desorption. The size of the dip progressively decreases and its location progressively moves towards the feed end of the reactor as more heat is supplied to the reactor from the shell side and by the hot purge steam. The entire reactor is heated up to ~550 °C at the end of this step.

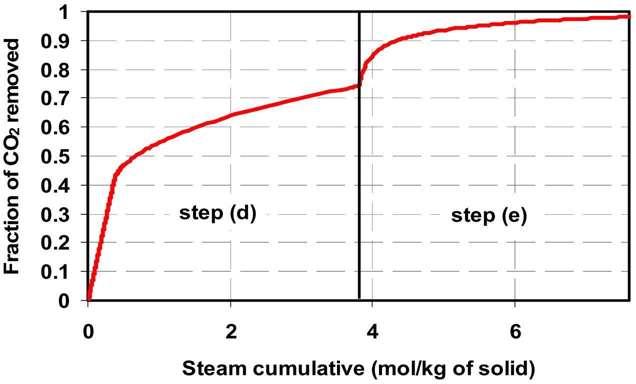

Fig. 14 Cumulative amount of steam purge and degree of regeneration

Figure 13 shows the specific CO_2 loading profiles inside the sorber-reactor at different times during step (e). The reactor is progressively cleaned of CO_2 during this step by purging with low pressure steam. The effluent gas contains dilute CO_2 mixed with steam and it is produced at a near ambient pressure which is wasted. The sorber contains very little CO_2 at the end of this step and a considerable section of the column near the H_2 product end (>35%) is free of CO_x. This degree of stringent cleaning of that end is necessary for production of fuel-cell grade H_2 during step (a).

Figure 14 provides an integrated view of the regeneration process by the proposed TSSER concept. It plots the fraction of CO_2 removed from the sorber-reactor during the regeneration steps (d) and (e) as a function of the cumulative amount of steam purge used in these steps. For example, Fig. 14 shows that the total specific amount of steam purge required to remove ∼98+% of total CO_2 from the sorber-reactor is ∼7.8 mol/kg of total solid. This is a rather moderate steam purge requirement by the process.

9 Over-all simulated TSSER process performance

The over-all simulated performance of the TSSER concept described above is summarized in Table 7. It compares the TSSER process performance at two feed gas pressures.

The remarkable process intensification by the proposed TSSER process is demonstrated by Table 7. The process directly produces a significant amount of fuel-cell grade H_2 from a synthesis gas feed ($CO:H_2O = 1:4$) at feed pressure with a high CO to H_2 conversion.

It should be noted that the conversion figure reported in Table 7 is the net conversion of CO to H_2 product by the proposed TSSER process. It is much higher than that can be achieved by the conventional route (Fig. 1) using a conventional PSA separation unit because the PSA process typically uses ∼15–25% of the H_2 product for its regeneration by back purge which significantly lowers the net CO to H_2 conversion even though the conversion in the WGS reactor may be high. The TSSER concept also directly produces an essentially pure CO_2 by-product with high recovery of total CO_2 produced. This gas is produced at a pressure which is much higher than the feed gas pressure. Thus, the process not only recovers the CO_2 produced by the WGS reaction, but also potentially lowers the subsequent cost and energy of its recompression for sequestration. These advantages are achieved because the WGS reaction and the product purification are simultaneously done in a single unit operation.

Another important result of the process simulation is the estimation of the steam duty for the regeneration of the chemisorbent. A very moderate amount of steam is needed to fully regenerate the chemisorbent (steps d and e). According to Table 7, the estimated cost of steam is only a small fraction (∼10–15%) of the cost of the H_2 product.

The operation of the TSSER process using the feed gas at 25 atm instead of 15 atm somewhat lowers the over-all performance, but the decrease may be acceptable. Higher pressure operation increases the amount of void gas containing H_2 at the end of the sorption-reaction step which reduces H_2 recovery. This problem may be rectified by recycling the step (b) effluent gas as feed. However, that dilutes the feed gas with H_2 and CO_2 which unfavorably shifts the equilibrium of the WGS reaction.

Table 7 Over-all simulated performance of the TSSER process

	Feed pressure = 15.0 atm	Feed pressure = 25.0 atm
Moles (net) of H_2 product per mole of CO in feed gas	0.933	0.894
High purity H_2 produced per cycle (<10 ppm CO)	0.71 mol/kg of solid Pressure ∼15.0 atm	0.72 mol/kg of solid Pressure ∼25.0 atm
Net CO_2 by-product produced (∼100% CO_2)	0.43 mol/kg of solid Pressure ∼33.0 atm	0.34 mol/kg of solid Pressure ∼45.3 atm
Net CO_2 recovery (% of total produced)	57.1	41.9
CO_2 removed from bed	∼74.2% (step d), ∼98.2% (step d + step e)	∼74.2% (step d), ∼98.5% (step d + step e)
Steam duty (steps d + e)	7.84 mol/kg of solid = 0.262 tons/MSCF H_2 product	8.01 mol/kg of solid = 0.262 tons/MSCF H_2 product
Cost of steam purge (steps d + e)	∼\$0.66* of steam/MSCF H_2 (*\$2.5/ton steam)	∼\$0.66* of steam/MSCF H_2 (*\$2.5/ton steam)

10 Summary

Two novel high temperature chemisorbents (K_2CO_3 promoted hydrotalcite and Na_2O promoted alumina) offer (i) reversible sorption of CO_2 in presence of steam, CO and H_2 with high selectivity in the temperature range of 250–450 °C, (ii) relatively fast and identical kinetics of sorption and desorption of CO_2, and (iii) moderate heats of sorption. A novel equilibrium isotherm model which accounts for simultaneous Langmuirian chemisorption of CO_2 on the sorbent surface and complexation of gaseous and chemisorbed CO_2 molecules can describe the isotherms on both chemisorbents at different temperatures.

A novel five-step thermal swing sorption enhanced reaction (TSSER) process concept is described which directly and simultaneously produces fuel-cell grade (<10 ppm CO) H_2 and pure ($\sim$99.9+%) compressed CO_2 from a synthesis gas ($CO + H_2O$) feed. The concept simultaneously carries out the reversible WGS reaction and chemisorption of CO_2 from the reaction zone in a single unit operation. The H_2 is produced at the feed gas pressure, and the CO_2 by-product is compressed by the process to much above that. The process offers very high conversion of CO to H_2 and high utilization of the CO_2 sorption capacity of the chemisorbent. The periodic regeneration of the chemisorbent is achieved by a two-stage steam purge. The total amount of steam needed for this purpose is relatively low.

Acknowledgements The work was partly supported by the Pennsylvania Infrastructure Technology Alliance grants (PITA-442-04 and PITA-542-5), by the U.S. Department of Energy under cooperative agreement DE-PS26-04NT-42454, and by a donation from Air Products and Chemicals, Inc.

References

Chakravarti, S., Gupta, A., Hunek, B.: Advanced technology for the capture of CO_2 from flue gases, First National Conference on Carbon Sequestration, Washington, DC, May 15–17 (2001)

Chue, K.T., Kim, J.N., Yoo, Y.J., Cho, S.H., Yang, R.T.: Comparison of activated carbon and zeolite 13X for CO_2 recovery from flue gas by pressure swing adsorption. Ind. Eng. Chem. Res. **34**, 591–598 (1995)

Ding, Y., Alpay, E.: Adsorption-enhanced steam-methane reforming. Chem. Eng. Sci. **55**, 3929–3940 (2000)

Fuderer, A., Rudelstorfer, E.: Selective adsorption of gases. U.S. Patent No 3,986,849 (1976)

Hufton, J.R., Mayorga, S., Sircar, S.: Sorption-enhanced reaction process for hydrogen production. AIChE J. **45**, 248–256 (1999)

Hufton, J.R., Weigel, S.J., Waldron, W.F., Rao, M., Nataraj, S., Sircar, S., Gaffney, T.R.: Sorption enhanced reaction process for production of hydrogen. DOE Report DE-FC36-95G010059 (2000)

IEA Greenhouse Gas R&D Programme: Carbon Dioxide Capture from Power Stations. Cheltenham, United Kingdom (1990)

Karasaki, M., Iijima, M., Shigeaki, M.: Removal of CO_2 from flue gases. Japanese Patent No 7,313,840 (1995)

Koros, W.J., Chern, R.T.: Separation of gas mixtures using polymeric membranes. In: Rousseau, R.W. (ed.) Handbook of Separation Process Technology, pp. 862–953. Wiley InterScience, New York (1987)

Leci, C.L., Goldthorpe, S.H.: Assessment of CO_2 removal from power station flue gas. Energy Convers. Manag. **33**, 477–485 (1992)

Lee, K.B., Beaver, M.G., Caram, H.S., Sircar, S.: Novel thermal swing sorption enhanced reaction process concept for hydrogen production by low temperature steam methane reforming. Ind. Eng. Chem. Res. **46**, 5003–5014 (2007a)

Lee, K.B., Verdooren, A., Caram, H.S., Sircar, S.: Chemisorption of carbon dioxide on potassium-carbonate-promoted hydrotalcite. J. Colloid Interface Sci. **308**, 30–39 (2007b)

Lee, K.B., Beaver, M.G., Caram, H.S., Sircar, S.: Chemisorption of carbon dioxide on sodium oxide promoted alumina. AIChE J. (2007c, in press)

Levenspiel, O.: Chemical Reaction Engineering: An Introduction to the Design of Reactors. Wiley, New York (1962)

Matsumoto, H., Kitamura, H., Kamata, T., Nishikawa, N., Ishibashi, M.: Fundamental study of CO_2 removal from thermal power plant flue gas by hollow-fiber gas-liquid contactor. Kagaku Kogaku Ronbun. **18**, 804–812 (1992)

Mimura, T., Shimojo, S., Suda, T., Iijima, M., Mitsuoka, S.: Research and development on energy saving technology for flue gas carbon dioxide recovery and steam system in power plant. Energy Convers. Manag. **36**, 397–400 (1995)

National Research Council and National Academy of Engineering: The Hydrogen Economy: Opportunities, Costs, Barriers, and R&D Needs. The National Academic Press, Washington (2004)

Qunying, J., Sixun, L.: Method for continuously gasifying coal (coke) and purifying synthesis gas. Chinese Patent No 1,156,754 (1997)

Rase, H.F.: Chemical Reactor Design for Process Plants. Wiley, New York (1977)

Rosen, M.A., Scott, D.S.: An energy-exergy analysis of the Koppers-Totzek process for producing hydrogen from coal. Int. J. Hydrogen Energ. **12**, 837–845 (1987)

Schlinger, W.G., Kolaian, J.H., Quintana, M.E., Dorawala, T.G.: Texaco coal gasification process for production of clean synthesis gas from coke. Energy Prog. **5**, 234–238 (1985)

Sircar, S.: Separation of multi-component gas mixtures. U.S. Patent No 4,077,779 (1979)

Sircar, S.: Separation of methane and carbon dioxide gas mixtures by pressure swing adsorption. Sep. Sci. Technol. **23**, 519–529 (1988)

Sircar, S., Golden, C.M.A.: PSA process for removal of bulk CO_2 from a wet high temperature gas. U.S. Patent No 6,322,612 (2001)

Sircar, S., Kratz, W.C.: Simultaneous production of hydrogen and carbon dioxide from steam reformer off-gas by pressure swing adsorption. Sep. Sci. Technol. **23**, 2397–2415 (1988)

Sircar, S., Kumar, R., Anselmo, K.J.: Effects of column nonisothermality or non-adiabaticity on the adsorption breakthrough curves. Ind. Eng. Chem. Proc. Des. Dev. **22**, 10–15 (1983)

Sircar, S., Hufton, J.R., Nataraj, S.: Process and apparatus for the production of hydrogen by steam reforming of hydrocarbon. U.S. Patent No 6,103,143 (2000)

Stiegel, G.J., Ramezan, M.: An overview of the U.S. Department of Energy's gasification technology program. ACS Symp. Div. Fuel Chem. **48**, 402–404 (2003)

Viaswinkel, E.E., Posthuma, S.A., Zuideveld, P.L.: The Shell gasification technology offers clean solutions for refineries and utility companies. Inst. Chem. Eng. Symp. Ser. **143**, 81–90 (1997)

Waldron, W.E., Hufton, J.R., Sircar, S.: Production of hydrogen by cyclic sorption enhanced reaction process. AIChE J. **47**, 1477–1479 (2001)

Xu, J.G., Froment, G.F.: Methane steam reforming, methanation, and water gas shift: I. Intrinsic kinetics. AIChE J. **35**, 88–96 (1989)